



Journal of Advanced Research in Fluid Mechanics and Thermal Sciences

Journal homepage:

https://semarakilmu.com.my/journals/index.php/fluid_mechanics_thermal_sciences/index

ISSN: 2289-7879



Application of the Conjugate Gradient Method for Predicting Unknown Heat Flux in 2D Plat under Effect of Insulation

Ari Satmoko¹, Engkos Achmad Kosasih^{1*}, Muhammad Irfan Dzaky¹, Hairul Abral², Anhar Riza Antariksawan³, Andril Arafat⁴

¹ Department of Mechanical Engineering, Universitas Indonesia, Depok 16424, West Java, Indonesia

² Department of Mechanical Engineering, Universitas Andalas, Padang, Indonesia

³ Research Center for Accelerator Technology, National Agency for Research and Innovation, Yogyakarta, Indonesia

⁴ Department of Mechanical Engineering, Universitas Negeri Padang, Padang, Indonesia

ARTICLE INFO

Article history:

Received 8 July 2023

Received in revised form 6 October 2023

Accepted 14 October 2023

Available online 27 October 2023

Keywords:

Inverse heat conduction; conjugate gradient method; heat flux prediction; condition monitoring; insulation

ABSTRACT

When an anomaly is discovered during a thermal inspection of industrial equipment, the diagnosis of finding the heat source is made more difficult by the presence of heat insulation. The use of the Conjugate Gradient Method (CGM) to solve the unknown heat flux in Inverse Heat Conduction Problem (IHCP) under insulation condition has been discussed. This method is used to predict a heat flux by utilizing temperature data at any points of measurement. The study deals with the structure of 2D thin plate at steady state. A copper plate with a thickness of 1 mm is used as specimen. White glass wool is used to thermally insulate the plate on the back surface. An electrical heater is plate mounted and operated by varying the DC voltage. A datalogger with thermocouple sensors records plate temperature changes. Software for solving the IHCP based on the CGM was developed. Initially, the software was implemented using synthetic data obtained from the forward heat conduction equations with a known heat flux. Simulated measurement data are assumed to have high accuracy (± 0.1 °C). Determination of heat flux with the CGM gives very satisfactory results with a low error below 0.12%. The CGM was then applied using experimental data. With a measurement error of ± 0.5 °C, the computational stopping criterion can still be met satisfactorily. In real installations, equipment is sometimes partially or completely isolated. In the experiment, this phenomenon is simulated by varying the isolation area as follows: 0%, 25%, 50% and 100%. The results of the flux calculation are correlated with the real flux supplied by the electrical heater. Each type of insulation area has a similar curve. By obtaining the correlation equation, the equivalent heat flux from calculation to real and vice versa can be carried out.

1. Introduction

One of the maintenance models in industrial installations is preventive maintenance which can be in the form of periodic maintenance or predictive maintenance. Periodic maintenance includes

* Corresponding author.

E-mail address: kosri@eng.ui.ac.id

<https://doi.org/10.37934/arfmts.110.2.176191>

scheduled routine maintenance (machine cleaning, machine inspection, engine oiling, and also replacement of spare parts according to age). Predictive maintenance attempts to anticipate failures by analyzing trends in machine behavior or condition. This treatment, also called condition monitoring, aims to ensure the continuity of the production process. Information from the monitoring process can be used to predict potential equipment damage. Utne *et al.*, [1] proposed a monitoring method with a structured approach. One step is to evaluate suitable condition monitoring method. There are many types of condition monitoring methods, but none of them can detect all potential failures. Each method has advantages and limitations. The simplest inspection is a visual inspection. Hamid *et al.*, [2] examined the roof of the building using the Unmanned Aerial Vehicle (UAV). With this drone, some roof defects can be detected. Further evaluation leads to a classification of the degree of damage.

Various parameters such as temperature, pressure or performance can be used as condition parameters. Temperature is the most frequently observed parameter because all physical changes result in temperature changes. If the condition monitoring yields abnormal data, a diagnosis is made to find the cause of the anomaly. Based on the measurement data, an analysis is carried out to find out what causes it. For example, if there is a hot spot or temperature anomaly, then the question is what heat source is causing the anomaly. This problem is known as the inverse problem where the effect is known from the measurement, but the cause is unknown. The inverse problem involving heat transfer in solids is known as the Inverse Heat Conduction Problem (IHCP).

Condition monitoring can be done either by qualitative or quantitative inspection. The qualitative inspection aims only to detect the presence of thermal pathology, without taking into account the severity of the anomaly. If a thermal pathology is detected, the thermal inspection should be followed by a quantitative inspection which can classify the severity and/or characterize the physical nature of the anomaly.

Temperature monitoring can be carried out either by contact, for example with a thermocouple sensor, or non-contact using an infrared sensor. Regarding temperature measurement technology, the Infrared Thermography (IRT) was stated by Garrido *et al.*, [3] as the most effective monitoring tool for both qualitative and quantitative inspections. The IRT for inspection activities was reviewed by Usamentiaga *et al.*, [4]. Temperature monitoring techniques can be done either passively or actively. In passive technique, the object is observed without the addition of external heat which normally leads to a steady state. On the other hand, in active technique, external heat is added which can lead to steady or transient conditions. The additional heat sources can be stimulated by electric heaters, lamps, lasers, eddy currents, or others. The heating process can be constant, pulse, vibro/wave, lock-in, etc.

The IHCP in transient conditions has been extensively studied. Its application is widely used for various purposes: estimation of heat sources, estimation of heat transfer coefficients at contact surfaces, estimation of convection coefficients, applications for non-destructive tests (NDT), characterization of the thermal properties of materials, and others. The transient IHCP using infrared scanner was pioneered by Le Niliot and Gallet [5] with cement block specimens equipped with heating wires and modeled in 2D. Then, Bozzoli *et al.*, [6] used a thin copper plate as a specimen. Duda [7] uses a beam with vertical and horizontal heating on both sides. Huang and Chaing [8] used a 3D transient model to identify unknown heat source configurations with irregular and moving boundaries. Sanches *et al.*, [9] estimated the time-varying boundary heat flux in a thin plate. The heat generated in the machining process is also an object of research: the turning process by Deppermann and Kneer [10], drilling with lubrication by Tai *et al.*, [11,12] and dry drilling by Huang *et al.*, [13]. They succeeded in predicting the temperature distribution of the workpiece or drill bit. Recently, without using the inverse approach, Mohd *et al.*, [14] performed bone drilling experiments. A significant

difference was obtained between the simulated temperature data and experimental measurements using an infrared camera. The application of the transient IHCP to estimate the heat transfer coefficient was reviewed by Xian *et al.*, [15]. The phenomenon of heat transfer at contact surfaces was studied by several researchers [16-18]. Vu *et al.*, [19] investigated the process of printing non-isothermal glass. Helmig and Kneer [20] discussed heat transfer in rotary bearings. The IHCP is also used to evaluate convection heat transfer. Bozzoli *et al.*, [21] studied the effect of butterfly inserts on heat exchangers. Bozzoli *et al.*, [22] discussed a specimen in the form of a helicoidal spiral tube. Bozzoli *et al.*, [23] continued his work with grooved spiral pipe objects. The convection phenomena in corrugated hollow pipes were also numerically studied by Amina *et al.*, [24]. Huang *et al.*, [25,26] investigated finned tube heat exchangers. Mobtil *et al.*, [27] worked on similar object by utilizing infrared transparent materials. F. Baldani, *et al.*, [28] uses a flat plate flowing with wind. Huang *et al.*, [26] and Cattani *et al.*, [29] discussed forced convection. Meanwhile for NDT applications, Jinlong *et al.*, [30] characterized the size and depth of subsurface defects of CFRP (carbon fiber reinforced polymere) composite materials. Junyan *et al.*, [31] and Holland and Schiefelbein [32] investigated subsurface defects and identified heat diffusivity in CFRP. Liu *et al.*, [33] reconstruct complex shaped delamination defects in multi-layer metal structures. Junyan *et al.*, [31] and Doshvarpassand *et al.*, [34] reviewed an overview of the application of infrared thermography for the detection and characterization of corrosion defects in metal materials. The IHCP can also be used to characterize the heat properties of materials. Gaverina *et al.*, [35] analyzed the thermal diffusivity in the in-plane direction. Groz *et al.*, [36] used an inverse method based on thermographic data to estimate the thermal resistance and layer thickness. Halloua *et al.*, [37] proposed a fast and novel method that allows to estimate the thermal and physical properties of CFRP laminated composites.

Not only transient condition that offers research areas, the IHCP under steady conditions also attracts the attention of researchers. Nemirovsky and Mozgova [38] used the boundary element method (BEM) in 2D problem to estimate both temperature and heat flux at the unknown boundary. Temperature measurement data were obtained by simulating direct problem equation. The BEM was also used by Wang *et al.*, [39] to be combined with the Conjugate Gradient Method (CGM) and by Wang *et al.*, [40] to be combined with Tikhonov's iteration. Jin and Marin [41] presented the use of the Method of the Fundamental Solutions (MFS) to recover a heat source from measurement of boundary temperature and heat flux. Similar research using the radial basis functions approach was carried out by Kołodziej *et al.*, [42]. Furthermore, Yu *et al.*, [43] also predicted temperature and heat flux using the MFS. Marin [44] applied the zero-order Tikhonov function to two-dimensional functionally graded materials (FGM). Marin and Karageorghis [45] continued his work with the case of linear isotropic thermoelasticity. Mohebbi *et al.*, [46] used a combination of the finite difference method and the CGM to functionally graded materials (FGM). Two different types of material gradations are considered for the thermal conductivity of the FGM which varies spatially in the form of a square or an exponential. Huang and Lee [47] used a combination of commercial software based on the finite volume method and the CGM to simultaneously estimate six unknown internal surface heat fluxes. With the same method, Huang and He [48] continued their work to search for unknown spatially dependent surface heat flux.

With various prospectus potential applications, research on the IHCP in transient conditions, especially associated with the IRT for temperature measurement, is of great interest. However, the majority of this research is still carried out on a laboratory scale where the environment can be conditioned. The temperature measurements with high accuracy can then be obtained. However, in a real inspection at the site, various problems arise. The surrounding environment creates noise that is hard to remove. The surface properties of the object to be monitored tend to have irregular emissivity due to degradation processes due to various physical phenomena during their operating

life. The surface properties of the observed object tend to have irregular emissivity due to degradation processes during their operating life. The quantitative and transient inspection at the site by relying on temperature measurements using the IRT is then very difficult to do. In this case, temperature measurement with contact sensors is more feasible than with infrared sensors.

From the literature above, solving the transient IHCP by measuring temperature using IRT technology offers prospectus challenges in characterizing thermal phenomena. However, this technique is difficult to apply to real in situ inspection because of difficulties in measuring temperatures with high accuracy. Another obstacle that is often encountered in site inspections is the presence of thermal insulation. Besides obstructing temperature measurement, insulation also adds complexity to the phenomenon of heat transfer. In-situ thermal inspection by measuring temperature using contact sensors in steady state is more feasible. For this reason, we study the steady state IHCP to determine unknown flux using multi-point temperature measurements for the 2D thin plate problem. Temperature monitoring is carried out with thermocouple sensors. The steady state is easily obtained by operating the facility in normal condition. The influence of insulation is also discussed whether it affects the reliability of flux calculations.

2. Methodology

2.1 Experimental Setup

The test scheme and experimental settings are shown in Figure 1. The copper plate specimen has dimensions of $18.0 \times 15.2 \text{ cm}^2$ with a thickness of 1 mm. The plate is in a vertical position. On the back surface of the plate is installed an electric heater with the dimensions of $3.0 \times 2.0 \text{ cm}^2$. Five thermocouple sensors are provided. White glasswool is used to thermally insulate the plate on the back surface. The heater is turned on by varying the DC voltage. The datalogger, calibrated with high precision mercury thermometers $0 \sim 150 \text{ }^\circ\text{C}$, records changes in plate temperatures. The datalogger is also used to measure ambient temperature.

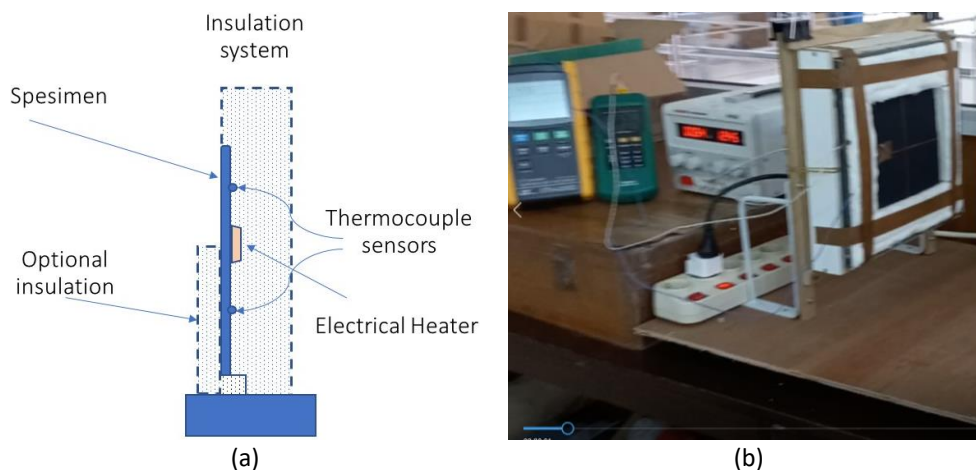
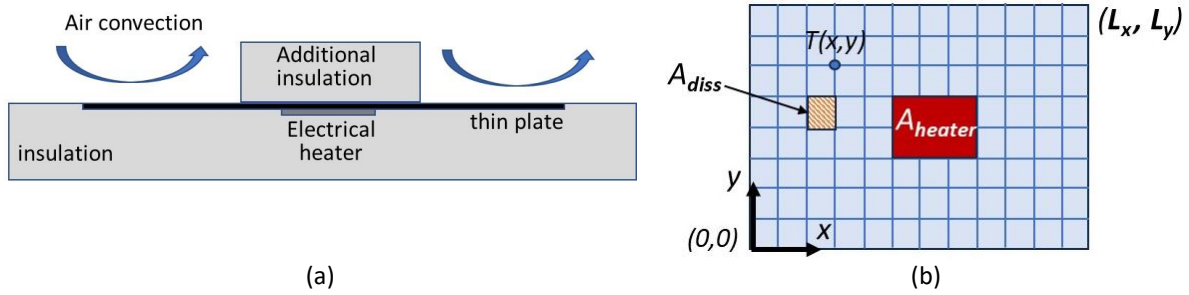


Fig. 1. (a) Test scheme and (b) experimental settings

2.2 Mathematical Model

A thin copper plate with the dimensions of thickness e , length L_x and width L_y has a thermal conductivity of k . An electric heater with a surface area of A_{heater} is placed at the center of the bottom surface of the plate (see Figure 2). The entire bottom surface of the plate is thermally isolated and the top surface allows air convection. An additional insulation is also installed on the top surface. The

insulation area is varied. The upper surface with the phenomenon of air convection or with insulation is denoted as A_{diss} . In fact, heat loss occurs from both above and bottom of the plate.



(a) (b)
Fig. 2. (a) Physical model and (b) plat model in 2D

The heat flux generated by the electric heater, q , is used to heat up the plate. Since the ambient temperature, T_a , is less than the plate temperature, $T(x,y)$, some of the heat is dissipated due to both air convection and imperfect insulation with a dissipation coefficient, h_{diss} . At steady state, the problem of heat transfer of the plate can be model by the following equations:

$$k \frac{\partial^2 T(x,y)}{\partial x^2} + k \frac{\partial^2 T(x,y)}{\partial y^2} + Q_{heater} - Q_{dissipation} = 0, \text{ for } 0 < x < L_x \text{ \& } 0 < y < L_y \quad (1)$$

$$Q_{heater} = A_{heater} q, \text{ for area } A_{heater} \quad (2)$$

$$Q_{dissipation} = A_{diss} h_{diss} (T(x, y) - T_a), \text{ for } A_{diss} \quad (3)$$

$$k \frac{\partial T(x,y)}{\partial x} = 0, \text{ for } x = 0 \text{ and } x = L_x \quad (4)$$

$$k \frac{\partial T(x,y)}{\partial y} = 0, \text{ for } y = 0 \text{ and } y = L_y \quad (5)$$

$$T(x, y) = T_i, \text{ for } x = x_i \text{ and } y = y_i \quad (6)$$

If the heat flux q is known, then the temperature distribution over the entire surface of the plate $T(x,y)$ can be calculated using Eq. (1) to Eq. (5). But in the inverse problem, Eq. (2) does not exist because the value of q is unknown. On the other hand, the temperature measurement at certain points is known according to (6).

The IHCP theory is discussed by Ozisik *et al.*, [49]. Temperature measurements carried out at certain points produce temperature data which, arranged in column vector form, becomes:

$$Y = (Y_1, Y_2, \dots, Y_i) \quad (7)$$

Every measurement is always accompanied by errors. If the error is additive by ϵ , then the result of Y measurement can be written as follows:

$$Y = T(q) + \epsilon \quad (8)$$

where $T(q)$ is the solution of the mathematical formulation of the heat transfer problem obtained from the parameter q .

Assuming that the measurement error is a Gaussian random variable, with a zero mean, known covariance and independent of the parameter q , then a probability density function can be developed leading finally to the maximum likelihood objective function, S_{ML} :

$$S_{ML}(q) = [Y - T(q)]^T [Y - T(q)] \quad (9)$$

In order for the objective function to be minimum, the Conjugate Gradient Method uses the following iterative procedure:

$$q^{k+1} = q^k - \beta^k d^k \quad (10)$$

where k is the iteration number, β^k is the search step size and d^k is the direction of descent. The direction of descent is the conjugation of the gradient direction, $\nabla S_{ML}(q^k)$ and the direction of descent of the previous iteration, d^{k-1} . It is given as

$$d^k = \nabla S_{ML}(q^k) + \gamma^k d^{k-1} \quad (11)$$

Through various assumptions and development of the Taylor series, the conjugation of the gradient direction is obtained as follows:

$$\nabla S_{ML}(q^k)^T = -2(J^k)^T [Y - T(q^k)] \quad (12)$$

where J is the sensitivity matrix:

$$J = [\partial T(q) / \partial q]^T \quad (13)$$

The flow chart for solving the unknown heat flux using the CGM algorithm is shown in Figure 3. The procedure starts with establishing a mathematical model. The forward problem is then executed with an initial guess of arbitrary heat flux as input. The results of temperature calculations are compared with measurement data. If the difference is still large, the initial guess is corrected with an iterative algorithm. The forward problem is re-evaluated with updated input guesses until finally the calculation results are close to the measured temperatures.

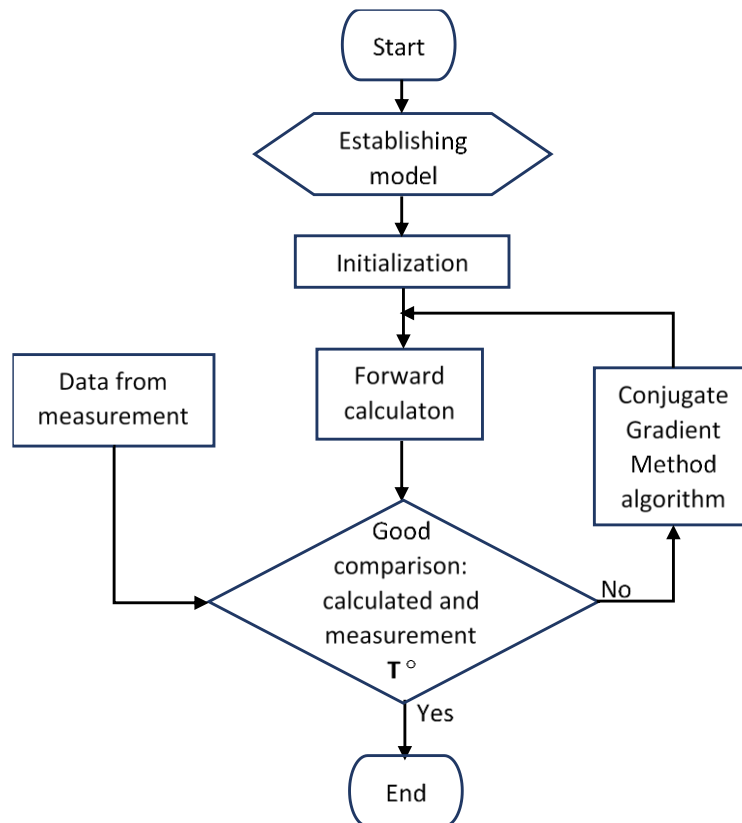


Fig. 3. Flowchart for resolving inverse problem

There are several criteria for stopping computation iterations and ensuring that the final guess matches the ideal solution. One way is to evaluate the S_{ML} variable with the following requirements:

$$S_{ML}(q^{k+1}) < \xi \quad (14)$$

where ξ is the fault tolerance. If the S_{ML} is small, it means that the $T(q^{k+1})$ solution is close to the measurement results.

Sensitivity coefficients are crucial parameter in guessing the flux. The central difference finite technique is used to evaluate the sensitivity coefficients J with the following equation:

$$J = [T(q^k + \epsilon q^k) - T(q^k)] / \epsilon q^k \quad (15)$$

where, q^k is the magnitude of the flux in the k -th iteration and ϵq^k is the finite difference step. For the stopping criteria, the residual between measured and estimated temperatures should be the same order of magnitude of the measurement errors, namely:

$$|Y_i - T(q^k)| \approx \sigma_i \quad (16)$$

where, σ_i is the standard deviation of the measurement error at point i . Assuming constant standard deviation (σ) and applying it to Eq. (9), $S_{ML}(q^{k+1})$ should be lower than ξ , that is:

$$\xi = n \sigma^2 \quad (17)$$

where n is the number of the measurement points.

3. Results

In accordance with the flowchart in Figure 2, a module for solving the forward problem is needed. The finite element method was developed by using 2D triangular elements with 3-nodes. The computation method was implemented in MATLAB software. By giving an arbitrary flux guess, the temperature distribution is obtained as an effect of the flux. The temperature calculated by the forward module is compared with the measured temperature. The flux guess is corrected by applying the Conjugate Gradient Method as discussed in the previous chapter.

3.1 Conjugate Gradient Method with Synthetic Data

The effectiveness of the Conjugate Gradient Method in predicting heat flux was first evaluated using synthetic simulation data. The copper plate is simulated by giving a heat flux of $7,100 \text{ W/m}^2$. The physical properties of the material are as follows: thermal conductivity of 385 W/m.K , density 8900 kg/m^3 and heat capacity 390 J/kg.C . The ambient temperature is $27 \text{ }^\circ\text{C}$, the coefficient of heat dissipation without insulation is $16.5 \text{ W/m}^2 \text{ C}$, and with insulation is $3.5 \text{ W/m}^2 \text{ C}$. The insulation area varies from 0%, 25%, 50% and 100% (Figure 4).

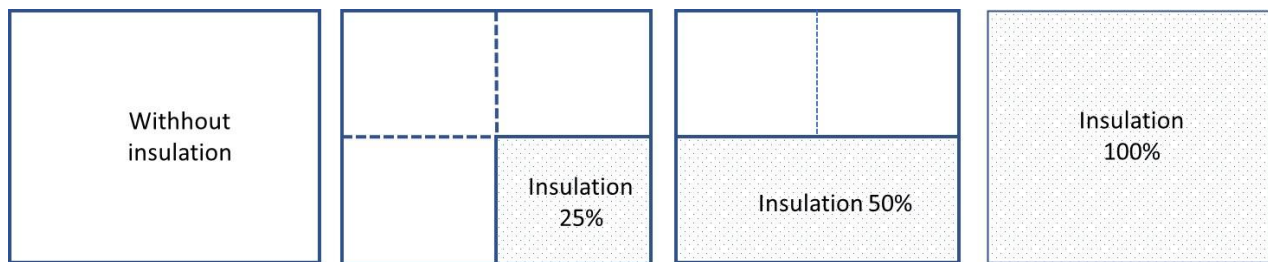


Fig. 4. Simulation with different insulation area

Insulation has the goal of preventing heat loss to the environment. This is clearly seen by increasing the steady-state temperature with the insulation area (see Table 1). The copper plate has high thermal conductivity, heat diffuses rapidly over the plate. The temperature difference between the maximum and minimum on the plate will not be much different, but can still be detected by the thermocouple sensor. The Table also shows that insulation also affects the minimum and maximum temperature differences on the plate.

Table 1
 Effect of the insulation area on plate temperatures with a heat flux of $7,100 \text{ W/m}^2$

No	Insulation area	Maximum temperature ($^\circ\text{C}$)	$\Delta T_{\text{min.max}}$ ($^\circ\text{C}$)
1	0 %	52.2	5.8
2	25%	57.4	6.7
3	50%	65.6	7.3
4	100%	118.4	5.9

To evaluate the accuracy in determining heat flux, the CGM method was evaluated using synthetic data. Temperature monitoring is assumed to be carried out at 4 arbitrary points (Figure 5). By using these 4 measurement points, the CGM method is applied to predict heat flux. Assume that the temperature measurement error (σ) is $\pm 0.1^\circ\text{C}$. The stopping criterion is then set to $\xi = 0.04$. Figure 6 shows the effectiveness of the CGM in predicting heat flux. As shown in Table 2, for all insulation

area variation, the heat flux prediction error is still below 0.15%. The accuracy of temperature measurement greatly determines the acceptance of heat flux prediction errors. If the measurement error was greater, the deviation of the heat flux calculation would also be greater.

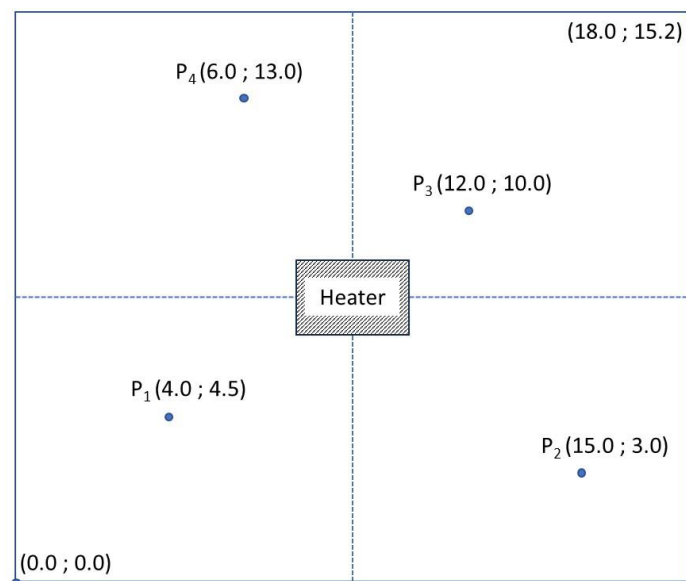


Fig. 5. Combination of 4 points for applying the CGM

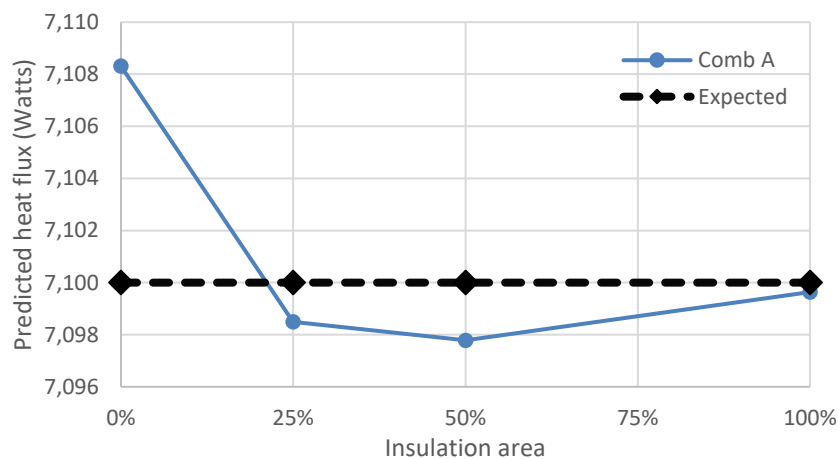


Fig. 6. The predicted heat flux in function of insulation area

Table 2

Calculated flux errors

No	Insulation area	Abs. error
1	0 %	0.12%
2	25%	0.02%
3	50%	0.03%
4	100%	0.01%
	Maximum	0.12%

3.2 Experimental Steady State Temperatures

In the experiment, temperature measurement was carried out by attaching 4 thermocouples to the plate. The locations of the 4 thermocouples are shown in Figure 7. Figure 8 shows the steady-state temperature as a function of the electric heating power for the case where no insulation is

applied on the front surface side. It is clear that the greater the applied electric heating power, the greater the steady state temperature.

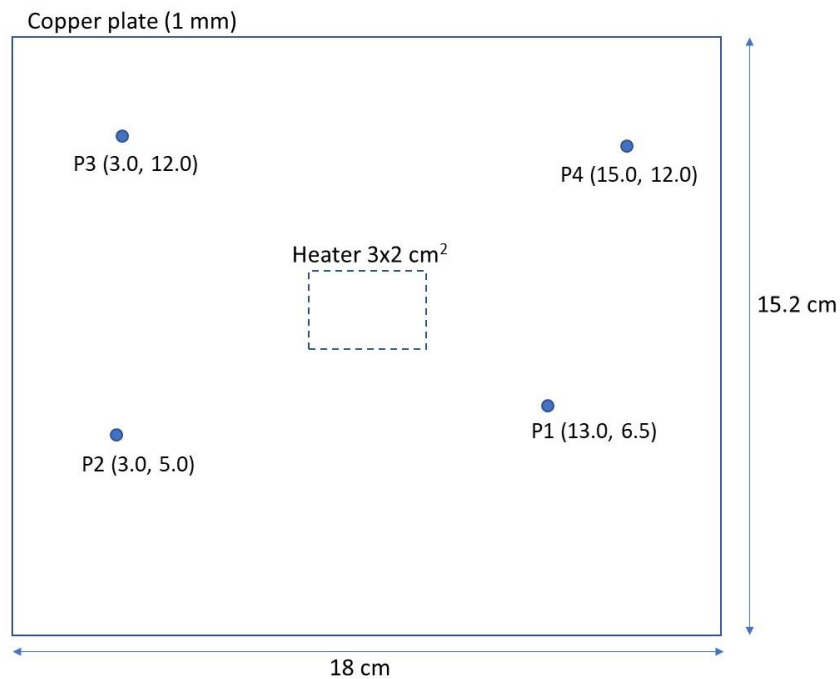


Fig. 7. Locations of thermocouples

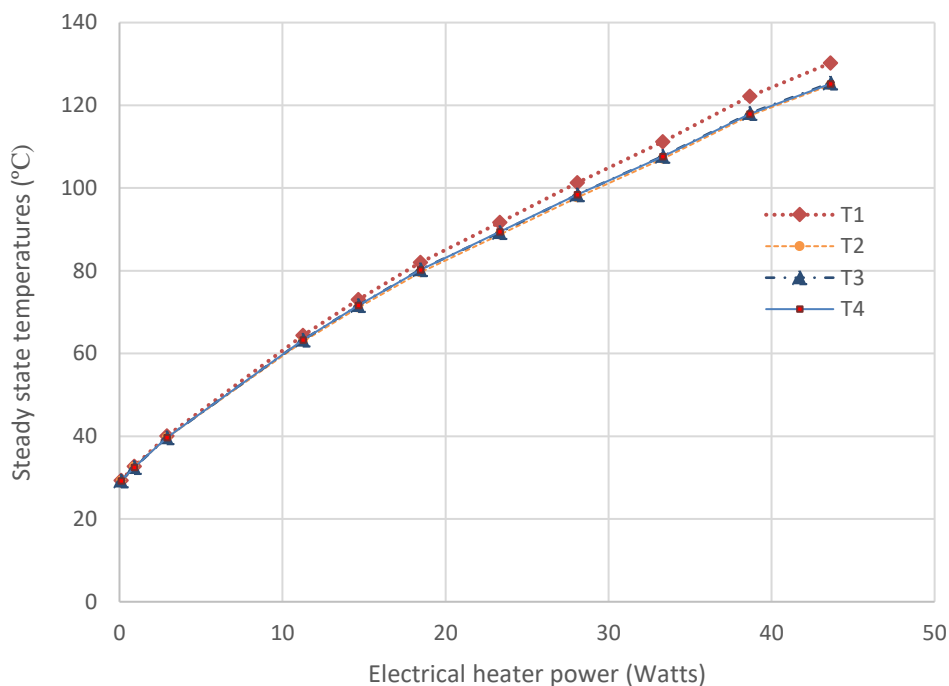


Fig. 8. Steady state temperatures without front face insulation

For measurements at point P1, the effect of insulation on steady state temperature is shown in Figure 9. The wider the insulation area, the more heat is absorbed by the plate. Without insulation, about 43 Watts of electric heating power is needed to reach a steady state at 130 °C. But with full insulation, it would take about 10 Watts to get the same steady state temperature.

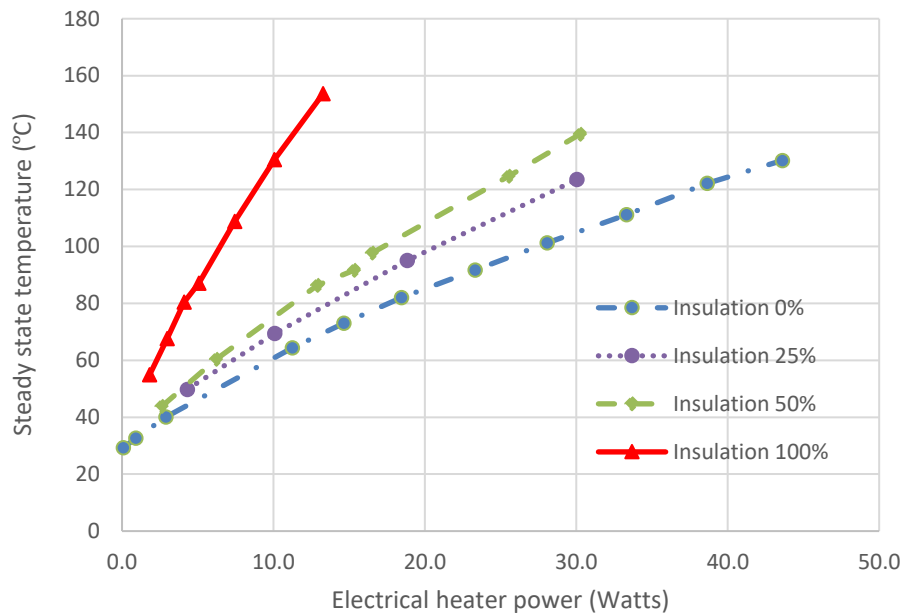


Fig. 9. Effect of heat insulation area on steady temperature at point P5

3.3 Characterization of Heat Loss

In Eq. (3), the parameter of the dissipation coefficient (h_{diss}) is required. This heat dissipation comes from either the top and bottom surfaces. This heat loss phenomenon is highly dependent on the test conditions. To characterize the heat loss, the copper plate is heated. After reaching steady state, the temperatures are recorded. Two tests were performed. Firstly, no insulation is provided on the front side of the plate. Secondly, the front side of the plate is completely insulated with 2 cm thick glass wool. The heat loss during steady state is assumed to be due to dissipated heat on both sides of the plate. That is equivalent to the heat supplied by the electrical heater. Figure 10 shows the heat loss as a function of the temperature difference between the plate temperature and the ambient temperature. The curves match well with second order polynomial regression. The heat transfer or dissipation coefficient representing the heat dissipated is required to solve the IHCP. Figure 11 shows the relationship between the dissipation coefficient and the temperature difference between the plate temperature and the ambient temperature. Without insulation on the front side of the plate, the logarithmic regression fits the experimental data. The logarithmic equation will then be used for approximation. With insulation, the curve tends to be linear. Instead of using linear regression, we use the same logarithmic equation as without insulation.

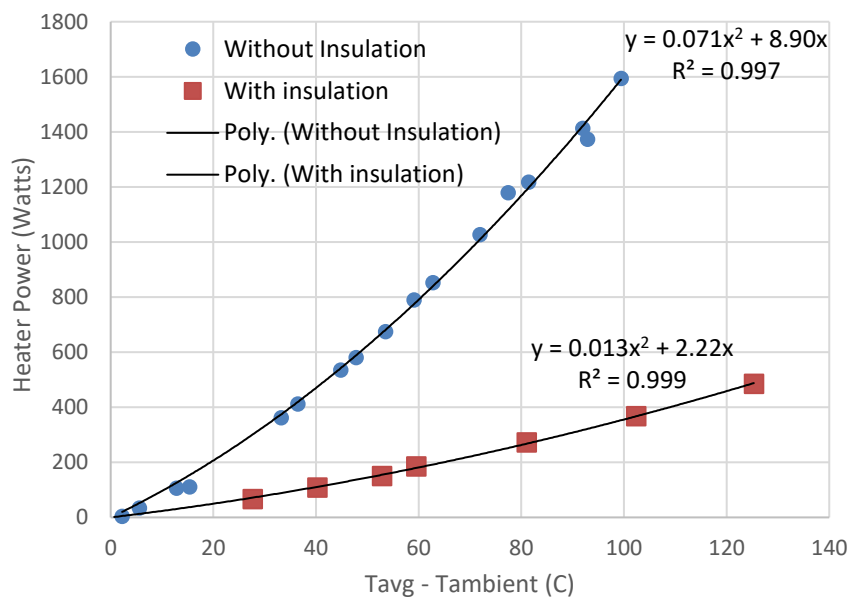


Fig. 10. The heat loss in function of the plate temperature

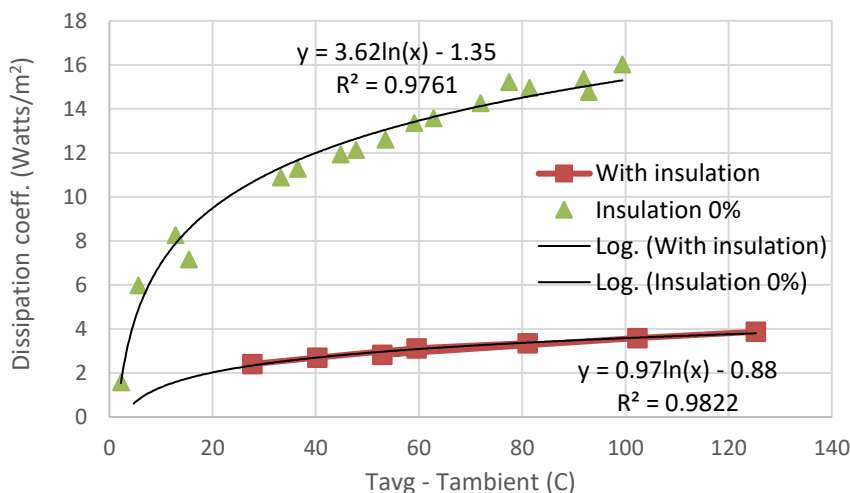


Fig. 11. Determination of the dissipation coefficient

3.4 Prediction of Experimental Heat Flux

By using the temperature measurements at steady state, the CGM method is applied to predict the heat flux supplied to the copper plate. Since the temperature measurement error is ± 0.5 °C, the stopping criteria $\xi = 4 \cdot 0.25 = 1.0$ is then used. Variation of insulation area is applied: 0%, 25%, 50%, and 100%. The calculated flux results are compared with the actual flux supplied by the electric heater (Figure 12). It shows 4 different curves according to the number of types of isolation areas. All curves have a similar trend. The correlation of the equation is given with the linear regression as shown in Table 3. By obtaining these equations, the conversion of the heat flux from calculation with the CGM to actual flux can be carried out or vice versa.

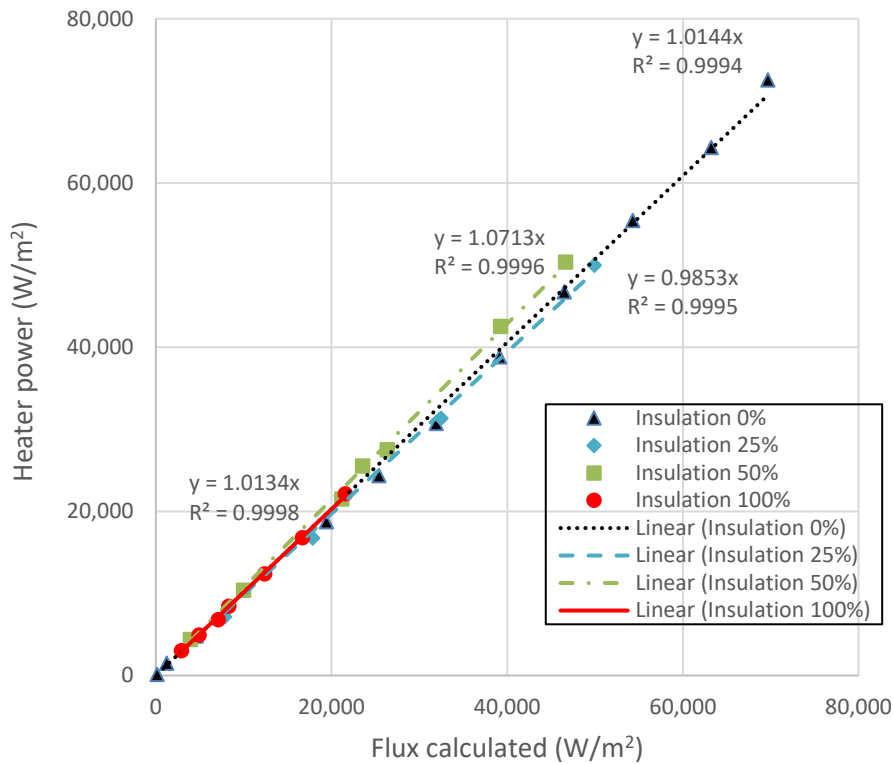


Fig. 12. Correlation between calculated and experimental heat flux

Table 3

Linear regression for correlation between experimental and calculated heat flux

No	Insulation area	Polynomial equation	R ² values
1	Insulation 0%	$y = 1.0144 x$	0.9994
2	Insulation 25%	$y = 0.9853 x$	0.9995
3	Insulation 50%	$y = 1.0713 x$	0.9996
4	Insulation 100%	$y = 1.0134 x$	0.9998

In all isolation conditions, the ratio between the experimental heater power and the calculated results is close to 1.00. This good curve is obtained by applying the heat dissipation coefficient value with a logarithmic approach. Approaches with linear or polynomial regression have also been tried and yielded unsatisfactory results. Thus, the key to the success of linear correlation is the use of the appropriate dissipation coefficient. Tests with insulation conditions of 25% and 50% were also carried out at lower temperatures compared to the lowest data dissipation coefficient with 100% insulation. That is, extrapolation in logarithmic regression equation regarding the dissipation coefficient gives satisfactory results.

4. Conclusions

The Conjugate Gradient Method for predicting unknown heat fluxes for 2D thin plate structures by using temperature measurements has been discussed. The calculation procedure begins by solving the forward conduction heat transfer equation. By providing an initial heat flux guess, the calculated temperature distribution of the structure is obtained and compared with the measurement data. If the difference is still large, the CGM algorithm regenerates the heat flux guess. The central finite difference technique is used to evaluate the sensitivity coefficients. The computational iteration is continued by updating the heat flux guess until it meets the stopping criteria.

To test the effectiveness of the CGM, synthetic data measurements are simulated. Assuming the temperature measurement error is ± 0.1 °C, the heat flux prediction error is still below 0.15%. The accuracy of temperature measurement greatly determines the acceptance of heat flux prediction errors. The combination of measurement points and the insulation area have practically no effect in predicting heat flux. The CGM is then used to predict the experimental heat flux. By using temperature measurement data, the CGM gives satisfactory results in predicting heat flux. Insulation results in a higher steady-state temperature than without insulation, but does not affect the precision of the heat flux calculation. The CGM managed to provide a linear correlation between the predicted and actual heat fluxes. The characterization of the test conditions, especially the heat dissipation coefficient determines the success of this correlation.

Acknowledgement

This research was funded by Riset Kolaborasi Indonesia 2022 (NKB-1068/UN2.RST/HKP.05.00/2022-23-06-2022).

References

- [1] Utne, I. B., T. Brurok, and H. Rødseth. "A structured approach to improved condition monitoring." *Journal of Loss Prevention in the Process Industries* 25, no. 3 (2012): 478-488. <https://doi.org/10.1016/j.jlp.2011.12.004>
- [2] Hamid, Nor Baizura, Masiri Kaamin, Noorul Hudai Abdullah, Mardiha Mokhtar, Siti Nooraiin Mohd Razali, Muhammad Naim Abu Bakar, Mohamad Ridhwan Zahri, and Nur Thaqifah Aina Mohd Zaidi. "Application of UAV and CSPI Matrix for Roof Inspection at Dewan Sultan Ibrahim and Dewan Tunku Mahkota Ismail UTHM." *Journal of Advanced Research in Applied Sciences and Engineering Technology* 28, no. 1 (2022): 106-115. <https://doi.org/10.37934/araset.28.1.106115>
- [3] Garrido, I., S. Lagüela, R. Otero, and P. Arias. "Thermographic methodologies used in infrastructure inspection: A review-Post-processing procedures." *Applied Energy* 266 (2020): 114857. <https://doi.org/10.1016/j.apenergy.2020.114857>
- [4] Usamentiaga, Rubén, Pablo Venegas, Jon Guerediaga, Laura Vega, Julio Molleda, and Francisco G. Bulnes. "Infrared thermography for temperature measurement and non-destructive testing." *Sensors* 14, no. 7 (2014): 12305-12348. <https://doi.org/10.3390/s140712305>
- [5] Le Niliot, Christophe, and Paulin Gallet. "Infrared thermography applied to the resolution of inverse heat conduction problems: recovery of heat line sources and boundary conditions." *Revue générale de Thermique* 37, no. 8 (1998): 629-643. [https://doi.org/10.1016/S0035-3159\(98\)80041-X](https://doi.org/10.1016/S0035-3159(98)80041-X)
- [6] Bozzoli, F., G. Pagliarini, and S. Rainieri. "Experimental validation of the filtering technique approach applied to the restoration of the heat source field." *Experimental Thermal and Fluid Science* 44 (2013): 858-867. <https://doi.org/10.1016/j.expthermflusci.2012.10.002>
- [7] Duda, Piotr. "A general method for solving transient multidimensional inverse heat transfer problems." *International Journal of Heat and Mass Transfer* 93 (2016): 665-673. <https://doi.org/10.1016/j.ijheatmasstransfer.2015.09.029>
- [8] Huang, Cheng-Hung, and Meng-Ting Chaing. "A transient three-dimensional inverse geometry problem in estimating the space and time-dependent irregular boundary shapes." *International Journal of Heat and Mass Transfer* 51, no. 21-22 (2008): 5238-5246. <https://doi.org/10.1016/j.ijheatmasstransfer.2008.03.019>
- [9] Sanches, Emerson L., Diego C. Knupp, Leonardo T. Stutz, Luiz AS Abreu, and Antônio J. Silva Neto. "Use of infrared thermography for the explicit heat flux estimation employing regularized measurements with truncated eigenfunction expansions." *Thermal Science and Engineering Progress* 26 (2021): 101084. <https://doi.org/10.1016/j.tsep.2021.101084>
- [10] Deppermann, Marc, and Reinhold Kneer. "Determination of the heat flux to the workpiece during dry turning by inverse methods." *Production Engineering* 9 (2015): 465-471. <https://doi.org/10.1007/s11740-015-0635-6>
- [11] Tai, Bruce L., David A. Stephenson, and Albert J. Shih. "An inverse heat transfer method for determining workpiece temperature in minimum quantity lubrication deep hole drilling." *Journal of Manufacturing Science and Engineering* 134, no. 2 (2012): 021006. <https://doi.org/10.1115/1.4005794>
- [12] Tai, Bruce L., David A. Stephenson, and Albert J. Shih. "Workpiece temperature during deep-hole drilling of cast iron using high air pressure minimum quantity lubrication." *Journal of Manufacturing Science and Engineering* 135, no. 3 (2013): 031019. <https://doi.org/10.1115/1.4024036>

- [13] Huang, Cheng-Hung, Li-Chun Jan, Rui Li, and Albert J. Shih. "A three-dimensional inverse problem in estimating the applied heat flux of a titanium drilling-Theoretical and experimental studies." *International Journal of Heat and Mass Transfer* 50, no. 17-18 (2007): 3265-3277. <https://doi.org/10.1016/j.ijheatmasstransfer.2007.01.031>
- [14] Mohd, Afza Nizam, Mohd Khairi Abu Husain, Shamsul Sarip, and Roslan Ismail. "Temperature Performance of Stainless Steel AISI420B Orthopedic Drill Bits Simulation Study." *Journal of Advanced Research in Applied Sciences and Engineering Technology* 26, no. 1 (2022): 78-96. <https://doi.org/10.37934/araset.26.1.7896>
- [15] Xian, Yaoqi, Ping Zhang, Siping Zhai, Peng Yuan, and Daoguo Yang. "Experimental characterization methods for thermal contact resistance: A review." *Applied Thermal Engineering* 130 (2018): 1530-1548. <https://doi.org/10.1016/j.applthermaleng.2017.10.163>
- [16] Fieberg, C., and R. Kneer. "Determination of thermal contact resistance from transient temperature measurements." *International Journal of Heat and Mass Transfer* 51, no. 5-6 (2008): 1017-1023. <https://doi.org/10.1016/j.ijheatmasstransfer.2007.05.004>
- [17] Burghold, E. M., Y. Frekers, and R. Kneer. "Transient contact heat transfer measurements based on high-speed IR-thermography." *International Journal of Thermal Sciences* 115 (2017): 169-175. <https://doi.org/10.1016/j.ijthermalsci.2017.01.019>
- [18] Helmig, Thorsten, Michael Burghold, Faruk Al-Sibai, and Reinhold Kneer. "Investigating the influence of macroscopic surface structures on the thermal contact conductance using infrared thermography." In *7th World Congress on Momentum, Heat and Mass Transfer*. 2020. <https://doi.org/10.11159/enfht20.166>
- [19] Vu, Anh Tuan, Anh Ngoc Vu, Gang Liu, Tim Grunwald, Olaf Dambon, Fritz Klocke, and Thomas Bergs. "Experimental investigation of contact heat transfer coefficients in nonisothermal glass molding by infrared thermography." *Journal of the American Ceramic Society* 102, no. 4 (2019): 2116-2134. <https://doi.org/10.1111/jace.16029>
- [20] Helmig, T., and R. Kneer. "A novel transient infrared-thermography based experimental method for the inverse estimation of heat transfer coefficients in rotating bearings." *International Journal of Thermal Sciences* 167 (2021): 107000. <https://doi.org/10.1016/j.ijthermalsci.2021.107000>
- [21] Bozzoli, F., L. Cattani, A. Mocerino, S. Rainieri, I. Tougri, and M. J. Colaço. "Characterisation of the heat transfer in displaced enhancement devices by means of inverse problem approach applied to IR images." *Quantitative InfraRed Thermography Journal* 18, no. 2 (2021): 108-126. <https://doi.org/10.1080/17686733.2019.1700696>
- [22] Bozzoli, Fabio, Luca Cattani, Sara Rainieri, and Giorgio Pagliarini. "Estimation of local heat transfer coefficient in coiled tubes under inverse heat conduction problem approach." *Experimental Thermal and Fluid Science* 59 (2014): 246-251. <https://doi.org/10.1016/j.expthermflusci.2013.11.024>
- [23] Bozzoli, Fabio, Luca Cattani, and Sara Rainieri. "Effect of wall corrugation on local convective heat transfer in coiled tubes." *International Journal of Heat and Mass Transfer* 101 (2016): 76-90. <https://doi.org/10.1016/j.ijheatmasstransfer.2016.04.106>
- [24] Amina, Mostefaoui, Saim Rachid, and Abboudi Saïd. "Numerical Analysis of The Thermo-Convective Behaviour of an Al₂O₃-H₂O Nanofluid Flow Inside a Channel with Trapezoidal Corrugations." *Journal of Advanced Research in Fluid Mechanics and Thermal Sciences* 89, no. 2 (2022): 114-127. <https://doi.org/10.37934/arfmts.89.2.114127>
- [25] Huang, Cheng-Hung, I-Cha Yuan, and Herchang Ay. "A three-dimensional inverse problem in imaging the local heat transfer coefficients for plate finned-tube heat exchangers." *International Journal of Heat and Mass Transfer* 46, no. 19 (2003): 3629-3638. [https://doi.org/10.1016/S0017-9310\(03\)00157-1](https://doi.org/10.1016/S0017-9310(03)00157-1)
- [26] Huang, Cheng-Hung, I-Cha Yuan, and Herchang Ay. "An experimental study in determining the local heat transfer coefficients for the plate finned-tube heat exchangers." *International Journal of Heat and Mass Transfer* 52, no. 21-22 (2009): 4883-4893. <https://doi.org/10.1016/j.ijheatmasstransfer.2009.05.023>
- [27] Mobtil, M., D. Bougeard, and S. Russeil. "Experimental study of inverse identification of unsteady heat transfer coefficient in a fin and tube heat exchanger assembly." *International Journal of Heat and Mass Transfer* 125 (2018): 17-31. <https://doi.org/10.1016/j.ijheatmasstransfer.2018.04.028>
- [28] Baldani, Francesco, Walter Bosschaerts, Souad Harmand, and Tony Arts. "Low speed numerical and experimental validation of a solving methodology for the inverse heat conduction problem by means of quantitative infra-red thermography." In *10th European Conference on Turbomachinery Fluid dynamics & Thermodynamics*. European Turbomachinery Society, 2013.
- [29] Cattani, Luca, Denis Maillet, Fabio Bozzoli, and Sara Rainieri. "Estimation of the local convective heat transfer coefficient in pipe flow using a 2D thermal quadrupole model and truncated singular value decomposition." *International Journal of Heat and Mass Transfer* 91 (2015): 1034-1045. <https://doi.org/10.1016/j.ijheatmasstransfer.2015.08.016>
- [30] Jinlong, Gong, Liu Junyan, Wang Fei, and Wang Yang. "Inverse heat transfer approach for nondestructive estimation the size and depth of subsurface defects of CFRP composite using lock-in thermography." *Infrared Physics & Technology* 71 (2015): 439-447. <https://doi.org/10.1016/j.infrared.2015.06.005>

- [31] Junyan, Liu, Wang Fei, Liu Yang, and Wang Yang. "Inverse methodology for identification the thermal diffusivity and subsurface defect of CFRP composite by lock-in thermographic phase (LITP) profile reconstruction." *Composite Structures* 138 (2016): 214-226. <https://doi.org/10.1016/j.compstruct.2015.11.062>
- [32] Holland, Stephen D., and B. Schiefelbein. "Model-based inversion for pulse thermography." *Experimental Mechanics* 59 (2019): 413-426. <https://doi.org/10.1007/s11340-018-00463-2>
- [33] Liu, Haochen, Cuixiang Pei, Shejuan Xie, Yong Li, Yifan Zhao, and Zhenmao Chen. "Inversion technique for quantitative infrared thermography evaluation of delamination defects in multilayered structures." *IEEE Transactions on Industrial Informatics* 16, no. 7 (2019): 4592-4602. <https://doi.org/10.1109/TII.2019.2950808>
- [34] Doshvarpassand, Siavash, Changzhi Wu, and Xiangyu Wang. "An overview of corrosion defect characterization using active infrared thermography." *Infrared Physics & Technology* 96 (2019): 366-389. <https://doi.org/10.1016/j.infrared.2018.12.006>
- [35] Gaverina, L., J. C. Batsale, A. Sommier, and Christophe Pradere. "Pulsed flying spot with the logarithmic parabolas method for the estimation of in-plane thermal diffusivity fields on heterogeneous and anisotropic materials." *Journal of Applied Physics* 121 (2017): 115105. <https://doi.org/10.1063/1.4978919>
- [36] Groz, M. M., A. Sommier, E. Abisset, S. Chevalier, J. L. Battaglia, J. C. Batsale, and Christophe Pradere. "Thermal resistance field estimations from IR thermography using multiscale Bayesian inference." *Quantitative InfraRed Thermography Journal* 18, no. 5 (2021): 332-343. <https://doi.org/10.1080/17686733.2020.1771529>
- [37] Halloua, Hicham, Abdellatif Obbadi, Youssef Errami, Smail Sahnoun, and Ahmed Elhassnaoui. "Nondestructive inverse approach for determining thermal and geometrical properties of internal defects in CFRP composites by lock-in thermography." In *2016 International Conference on Electrical Sciences and Technologies in Maghreb (CISTEM)*, pp. 1-7. IEEE, 2016. <https://doi.org/10.1109/CISTEM.2016.8066828>
- [38] Nemirovsky, Y. V., and A. S. Mozhgova. "Two-dimensional steady-state heat conduction problem for heat networks." In *Journal of Physics: Conference Series*, vol. 1359, no. 1, p. 012138. IOP Publishing, 2019. <https://doi.org/10.1088/1742-6596/1359/1/012138>
- [39] Wang, Shoubin, Li Zhang, Xiaogang Sun, and Huangchao Jia. "Solution to two-dimensional steady inverse heat transfer problems with interior heat source based on the conjugate gradient method." *Mathematical Problems in Engineering* 2017 (2017). <https://doi.org/10.1155/2017/2861342>
- [40] Wang, Fajie, Wen Chen, Wenzhen Qu, and Yan Gu. "A BEM formulation in conjunction with parametric equation approach for three-dimensional Cauchy problems of steady heat conduction." *Engineering Analysis with Boundary Elements* 63 (2016): 1-14. <https://doi.org/10.1016/j.enganabound.2015.10.007>
- [41] Jin, Bangti, and Liviu Marin. "The method of fundamental solutions for inverse source problems associated with the steady-state heat conduction." *International Journal for Numerical Methods in Engineering* 69, no. 8 (2007): 1570-1589. <https://doi.org/10.1002/nme.1826>
- [42] Kołodziej, Jan Adam, Magdalena Mierzwićzak, and Michał Ciałkowski. "Application of the method of fundamental solutions and radial basis functions for inverse heat source problem in case of steady-state." *International Communications in Heat and Mass Transfer* 37, no. 2 (2010): 121-124. <https://doi.org/10.1016/j.icheatmasstransfer.2009.09.015>
- [43] Yu, Guang Xu, Jie Sun, Hua Sheng Wang, Pi Hua Wen, and John W. Rose. "Meshless inverse method to determine temperature and heat flux at boundaries for 2D steady-state heat conduction problems." *Experimental Thermal and Fluid Science* 52 (2014): 156-163. <https://doi.org/10.1016/j.expthermflusci.2013.09.006>
- [44] Marin, Liviu. "Numerical solution of the Cauchy problem for steady-state heat transfer in two-dimensional functionally graded materials." *International Journal of Solids and Structures* 42, no. 15 (2005): 4338-4351. <https://doi.org/10.1016/j.ijsolstr.2005.01.005>
- [45] Marin, Liviu, and Andreas Karageorghis. "The MFS for the Cauchy problem in two-dimensional steady-state linear thermoelasticity." *International Journal of Solids and Structures* 50, no. 20-21 (2013): 3387-3398. <https://doi.org/10.1016/j.ijsolstr.2013.06.006>
- [46] Mohebbi, Farzad, Ben Evans, and Timon Rabczuk. "Solving direct and inverse heat conduction problems in functionally graded materials using an accurate and robust numerical method." *International Journal of Thermal Sciences* 159 (2021): 106629. <https://doi.org/10.1016/j.ijthermalsci.2020.106629>
- [47] Huang, Cheng-Hung, and Chien-Tsuen Lee. "An inverse problem to estimate simultaneously six internal heat fluxes for a square combustion chamber." *International Journal of Thermal Sciences* 88 (2015): 59-76. <https://doi.org/10.1016/j.ijthermalsci.2014.08.021>
- [48] Huang, Cheng-Hung, and Kai-Jyun He. "A steady-state inverse heat conduction-convection conjugated problem in determining unknown spatially dependent surface heat flux." *Case Studies in Thermal Engineering* 39 (2022): 102411. <https://doi.org/10.1016/j.csite.2022.102411>
- [49] Ozisik, M. Necat, H. R. B. Orlande, and A. J. Kassab. "Inverse Heat Transfer: Fundamentals and Applications." *Applied Mechanics Reviews* 55, no. 1 (2002): B18-B19. <https://doi.org/10.1115/1.1445337>